Supplementary Materials

Designing of Zn(II)-isonicotinohydrazido thiophenyl based 2D coordination polymer: structure, augmented photoconductivity and superior biological activity

Kingshuk Debsharma, Sunanda Dey, Dhananjoy Das, Satyajit Halder, Joaquin Ortega-Castro, Sarita Sarkar, Basudeb Dutta, Suvendu Maity, Kuladip Jana*, Antonio Frontera,* Partha Pratim Ray* and Chittaranjan Sinha*

Table of Contents

Experimental Section

Materials and methods

Isoniazid (TCI, AR grade), thiophen-2-carbaldehyde (Sigma Aldrich) and $Zn(NO_3)_2 \cdot 6H_2O$ (Sigma Aldrich) were used without further purification in the synthesis of the compounds. The elemental analysis (C, H and N) was taken from PerkinElmer 2400 elemental analyzer. To know thermal stability of the synthesized compound, thermogravimetric analyses were recorded on a PerkinElmer Pyris Diamond TG/DTA with the temperature range between 30-700 °C under a N_2 atmosphere through heating rate of 12 °C min^{-1}. Phase purity of the compound in bulk was measured by PXRD data from Bruker D8 ADVANCE X-ray diffractometer with CuKα radiation (λ, 1.548 Å). The optical characterization of the synthesized compound was taken by Shimadzu 2401 PC UV−Vis spectrophotometer (200−900 nm). For biological application DCFDA (#D6883) was purchased from Sigma-Aldrich (India). Fetal bovine serum (#16000044) was obtained from Gibco, USA and MEM sodium pyruvate, MEM non-essential amino acids L-glutamine and Gentamicin, were procured from Hi-Media, India.

Synthesis of the compound

The N, O-donor Schiff base, (E)-N'-(thiophen-2-ylmethylene)isonicotinohydrazide (HSIZ) was prepared from the reaction of isoniazid and thiophene-2-carbaldehyde by stirring for 6 h in dry MeOH.[1] The resultant solution of HSIZ (0.046 g, 0.2 mmol) in DMF/MeOH (1:10, 2 mL) was slowly layered in a solution of $Zn(NO)_3 \cdot 6H_2O$ (0.03 g, 0.1 mmol), in H_2O (2 mL) using 2 mL of buffer solution (1:1, v/v, MeOH:H_2O) (**Scheme S1**). The brown colored prismatic crystal of the compound $\{[Zn(SIZ)_2].DMF\}_n$ (CP**1**) were obtained after seven days (0.0402 g, yield: 67%). Elemental analysis (%) for $C_{25}H_{24}N_7O_3S_2Zn$; calcd: C 50.04, H 4.03, N 16.34; found: C 50.00, H 4.01, N 16.38. As the used amount of starting materials is increased, the yield of the CP is almost

constant. If the quantities of all the starting material have enhanced as per their molar ratios then the percentage of yield will be nearly unchanged but the quantity of the crystalline product can be increased. Every time the same material has been obtained when we have used the same amount of starting materials repeatedly; reproducibility of the material is very much satisfactory.

X-ray Crystallography

Brown coloured prismatic single crystal of the compound, CP**1**, was taken for data collection from Bruker SMART APEX II[2] diffractometer equipped with graphite-monochromated MoKα radiation (λ, 0.71073 Å). To determine the unit cell parameters and crystal-orientation matrices, least squares refinements of all reflections with hkl range -18<h<18, -16<k<16, -14<l<14 was used. The intensity of data were corrected for Lorentz and polarization effects.[3] The crystal data were collected in accordance with the condition of I>2σ (I). All the calculations for crystal structure were carried out using SHELXL -2016/6,[4] ORTEP-3,[5] and PLATON 99,[6] programs. The crystal structure was refined using DMF as a solvent model. But, it is symmetry generated, so, in the grow structure; DMF appears as twice like a mirror image. Hence, the DMF unit was refined with its 50% occupancy. All the non-hydrogen atoms of the compound were refined by anisotropic thermal parameters. Crystal parameters and some selected bond lengths with bond angles are reported in **Tables S1** and **S2**.

Device fabrication

A Schottky diode equipped with MS junction was devised for getting an idea about different charge conduction parameters of the synthesized compound. Accordingly, a thorough and careful cleaning of ITO coated glass substrate was performed sequentially with 2-propanol, acetone and distilled water respectively. Side-by-side, a well-dispersed medium comprised of the synthesized compound was prepared parallelly in DMF upon ultra-sonicating the system for 1 h. Thereafter,

the developed well-dispersed and sonicated medium was allowed to be spin-coated onto the ITO substrate for 2 minutes using SCU 2700 spinning unit with the coating rate of 800 rpm, followed by vacuum dried the as-prepared film having a thickness of ~ 1 μm in an oven. Finally, a Vacuum Coating Unit (12A4D) of HindHivac was employed for pressure-induced deposition of aluminum electrode at ~ 10^{-6} Torr as the metal contact. Evidently, the effective Schottky contact area through the deposition of the shadow mask was calculated to be 7.065×10^{-6} m^{-2}.

Solid state calculations

The program series from Cambridge Serial Total Energy Package (CASTEP) of Accelrys, Inc was encoded for optimizing the *C*2/*c* monoclinic crystal via the Density Functional Theory (DFT) calculation.[7] The relaxation parameters of all the atoms in 2D coordination polymer were fixed with the unit cell parameters, obtained experimentally. The Generalized Gradient Approximations (GGA); Perdew-Burke-Ernzerhof (PBE) functional[8,9] and ultrasoft pseudopotentials[10] with the relativistic treatment of the Koelling-Harmon[11] were used. A plane-wave basis set (340 eV cutoff) in the Γ points over the Brillouin zone were used. During all the calculations, the tolerance for the self-consistent field (SCF) was energetically converged to 1×10^{-6} eV/atom. The Grimme scheme with the dispersion corrected DFT-D have been included in the calculations.[12] Norm-conserving pseudo-potentials with a cutoff of 750 eV were used for the property's calculations. Band structures of the crystal were calculated in the first Brillouin zone along the k-vector, and the density of the states, regarding the Fermi level were plotted both totally (TDOS) as well as partially (PDOS) using a 2×2×2 grid. A specifically directed plane polarized light along the polarization coordinates of (100) (010) (001) were used to measure different optical properties of the crystal namely dielectric function as well as optical conductivity. The engaged smearing energy was kept as 0.2 eV.

To calculate the linear response of vertically excited electronic energy in synthesized CP at its first excited state, the energy minimized geometry was directly computed by CASTEP-encrypted time-dependent density functional theory (TD-DFT) based on the work of Hutter.[13]

TD-DFT section

Electronic excitation energies of the first six energy levels and optimized geometry of the first excited state were calculated with time-dependent density functional theory (TD-DFT) implemented in CASTEP. The Generalized Gradient Approximations (GGA) join to Perdew-Burke-Ernzerhof (PBE) functional[8,9] were used. Norm-conserving pseudo-potentials with a cutoff energy of 750 eV in the Γ points over the Brillouin zone with the relativistic treatment of the Koelling-Harmon[11] were employed. The tolerance for the self-consistent field (SCF) was energetically converged to 1×10^{-6} eV/atom. The Grimme scheme with the dispersion corrected DFT-D have been included in the calculations.[12] The implementation of TD-DFT in CASTEP followed the work of Hutter[13], which takes a linear response approach to computing excitation energies directly.

Frontier Orbital calculation

Molecular orbital calculations taken as a starting point before optimizations were performed with the double numerical with polarization (DNP) basis set[14] in the all-electron scheme, Γ point set and PBE functional[8,9] using the Dmol3 program code of Accelrys, Inc.

Microbial studies

A Gram-positive human pathogen, *Staphylococcus aureus* and Gram-negative *Escherichia coli* were used in this study. This organism was grown in LB (Luria Bertani) broth at 37 °C for 24 h. The media was prepared in sterilized double distilled water at pH, 7.0.

MIC determination

The broth dilution method was used to determine the MIC of CP**1** against *Staphylococcus aureus* and *Escherichia coli*.[15] For this purpose, 50 µL of a saturated overnight grown fresh culture of *Staphylococcus aureus* and *Escherichia coli* was individually added to different sterile test tubes containing 5 ml of sterile LB (Luria Bertani) media. After that, different concentrations of CP**1** (10, 20, 40, 60, 80 µg/ml) were added separately to the test solutions. However, the CP**1** was not added to the control; the organism was allowed to grow in the LB media. Thereafter, all the test tubes were incubated at 37°C for 24 h. The turbidity was checked by measuring OD at 600 nm and MIC was determined at the minimum concentration of CP**1** where no visible microbial growth was found.

MBC determination

This experiment was used to assess the bactericidal concentration of CP**1** against the gram-positive pathogen, *Staphylococcus aureus*. However, to start this experiment, 100 µL from each tube of different concentrations of CP**1** (10, 20, 40, 60, 80 µg/ml) of previous experiment was poured and spread onto several sterile LA (Luria Bertani Agar) plate. Thereafter, all the plates including control were incubated. Then the bacteria were allowed to multiply on agar plate at 37°C for 24 h.

Anti-cancer study

Four cancer cell lines, HCT-116 (Colon cancer), HeLa (Cervical cancer), MDA-MB-231 (human breast cancer cell), HepG2 (hepatocellular carcinoma) and human normal kidney epithelial cell line, NKE were obtained from Bose Institute, Kolkata. All the above cell lines were cultured using DMEM or RPMI medium, supplemented with 10% FBS, non-essential amino acids, 1 mM

sodium pyruvate, 2 mM L-glutamine, 100 mg/L streptomycin, 100 units/L penicillin, and 50 mg/L gentamycin in a 37°C humidified incubator containing 5% CO_2.

Cell survivability assay

Cell survivability of CP**1** studied on four cancer cell lines HCT-116, HeLa, MDA-MB-231, HepG2 as well as human normal kidney epithelial cell line, NKE using MTT assay.[16,17] Briefly cells were seeded in 96-well plates at 1×10^4 cells per well and exposed to synthesized compound, CP**1** at concentrations of 0-100 µg/mL for 24 h. Then the cells were washed with 1×PBS by twice and incubated with MTT solution (450 µg/mL) for 3-4 h at 37ºC. The resulting formazan crystals were dissolved in an MTT solubilization buffer and at 570 nm wavelength, the absorbance was measured and the value was compared with control cells.

Apoptosis assay

Induction of apoptosis was quantified via flow cytometric analysis using the Annexin V-FITC apoptosis detection kit (BD Bioscience).[18] The mechanistic study was done for HeLa cells because CP**1** had shown highest efficiency on this cancer cell line. The HeLa cells were seeded in a 6 well plate (density, 1×10^6 cells/mL) and post treatment control and CP**1** (5 µg/mL, 10 µg/mL, and 20 µg/mL) treated cells were trypsinized and re-suspended in 1X binding buffer solution (100 µL) and incubated with annexin V-FITC (5 µL) and PI (5 µL) for 15 min at room temperature in dark before acquiring data using BD FACS Verse flow cytometer (BD Biosciences, San Jose, CA). Annexin V/FITC positive cells were regarded as apoptotic cells analyzed using Cell Quest Software (BD Biosciences).

Measurement of cellular ROS

To estimate the intercellular reactive oxygen species (ROS) production due to CP**1** treatment, DCFDA method was used.[19] Briefly, HeLa cells were seeded in a 6 well plate and treated with

solution of CP**1** (5, 10, and 20 µg/mL) for 48 h time period and Etoposide was used as a standard control, post incubated with H_2DCFDA (10 µM) for 30 min at 37^{0}C. For fluorescent imaging, H_2DCFDA incubated cells were washed, resuspended in 1×PBS and directly imaged under fluorescent microscope (Leica).

Caspase 3/7 activation assay

Further to estimate the changes in caspase 3 protease activity of CP1 treated HeLa cells, caspase 3/7 assay (abcam) was used.[20] Cell lysates were prepared from HeLa cell treated with test compound (5 µg/mL, 10 µg/mL and 20 µg/mL) for 48h time period and aliquot of 150 µg of protein was used for each condition. DTT (10 mM) and DEVD-p-NA substrate (200 µM) were added according to manufactures protocol and incubated at 37°C for 2h. Finally optical density (OD) was measured at 400 nm in Thermo Multiskan GO microplate reader and the graph was plotted.

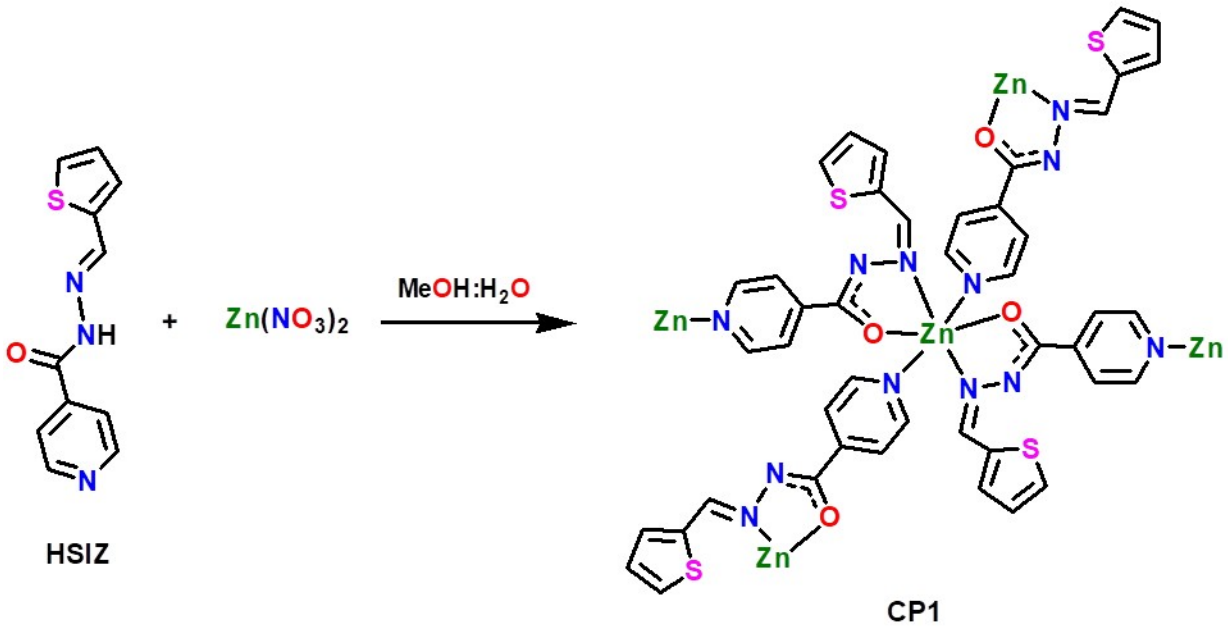

Scheme S1 Synthesis of CP**1** upon the reaction of $Zn(NO_3)_2$ with HSIZ ligand.

Table S1 Crystal data and refinement parameters for CP**1.**

Formula	$C_{25}H_{24}N_7O_3S_2Zn$
fw	600.00
crystal system	monoclinic
space group	*C*2/*c*
a (Å)	15.916(2)
b (Å)	13.6511(17)
c (Å)	12.5195(15)
$\alpha = \gamma$(deg)	90
β(deg)	107.201(4)
V (Å^3)	2598.4(6)
Z	4
D_{calcd}(g/cm^3)	1.534
μ(mm^{-1})	1.149
λ(Å)	0.71073
data[$I > 2\sigma(I)$]/params	2297/193
GOF on F^2	1.066
final *R* indices[$I > 2\sigma(I)$][a,b]	*R*1 = 0.0489 *wR*2 = 0.1385

[a]$R_1 = \Sigma||F_o|-|F_c||/\Sigma|F_o|$; [b]$wR_2 = \{\Sigma[w(F_o^2-F_c^2)^2]/\Sigma[w(F^2_o)^2]\}^{1/2}$; $w = [\sigma^2(F_o)^2 + (0.1003P)^2 + 4.9693P]^{-1}$ $(F_o^2 + 2F_c^2)/3$; [c]Goodness-of-fit

Table S2 Selected bond lengths and bond angles in CP**1.**

Zn(1) - O(1)	2.066(3)	Zn(1) - N(3)e	2.085(3)
Zn(1) - O(1)e	2.066(3)	Zn(1) - N(1)a	2.340(3)
Zn(1) - N(3)	2.085(3)	Zn(1) - N(1)d	2.340(3)
O(1) - Zn(1) - N(3)	77.86(12)	N(1)a - Zn(1) - O(1)e	92.58(11)
O(1) - Zn(1) - O(1)e	180.00	N(1)d - Zn(1) - N(3)e	86.66(12)
N(3) - Zn(1) - N(1)d	93.37(12)	O(1) - Zn(1) - N(1)d	92.58(11)
N(1)a - Zn(1) - N(1)d	180.00(16)	N(3) - Zn(1) - N(1)a	86.63(12)
N(1)d - Zn(1) - O(1)e	87.42(11)	N(3) - Zn(1) - N(3)e	180.00
O(1) - Zn(1) - N(1)a	87.42(11)	N(1)a - Zn(1) - N(3)e	93.37(12)
O(1) - Zn(1) - N(3)e	102.14(12)	O(1)e - Zn(1) - N(3)e	77.86(12)
N(3) - Zn(1) - O(1)e	102.14(12)	C(4) - N(1) - Zn(1)b	119.3(3)

Symmetry Code: a= x, -y, -1/2+z; b= x, -y, 1/2+z; d= 1/2-x, 1/2+y, 1/2-z; e= 1/2-x, 1/2-y, -z.

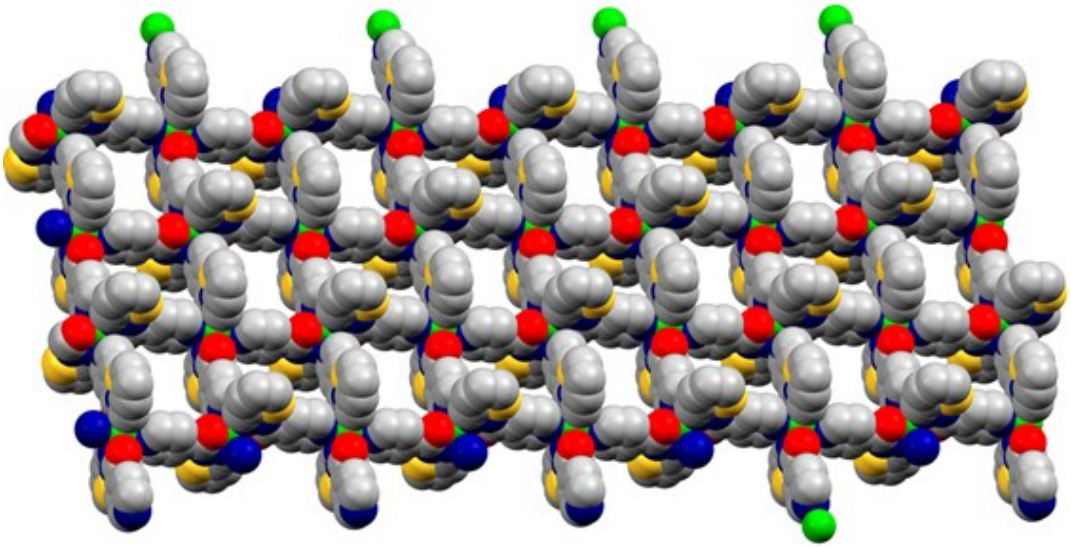

Fig. S1 Space-fill view of CP**1**.

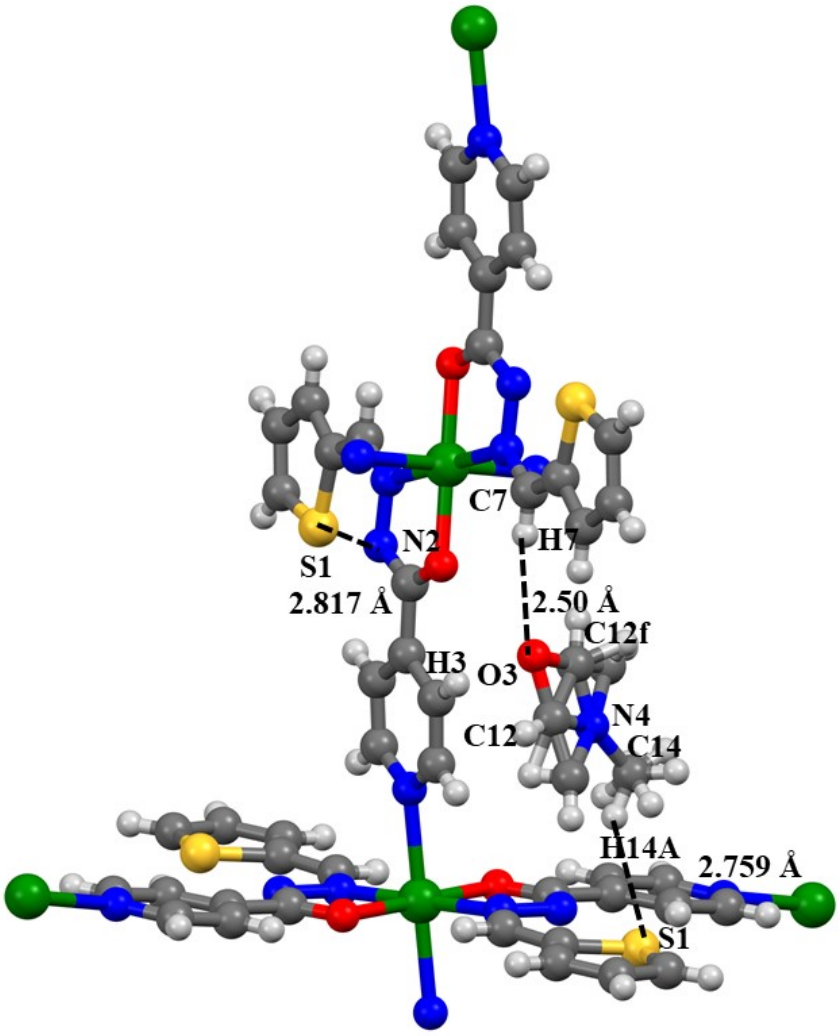

Fig. S2 Some noncovalent interactions in CP**1** (gray: C, blue: N, green: Zn, yellow: S, red: O, white: H, numerical value indicates there is a favorable interaction).

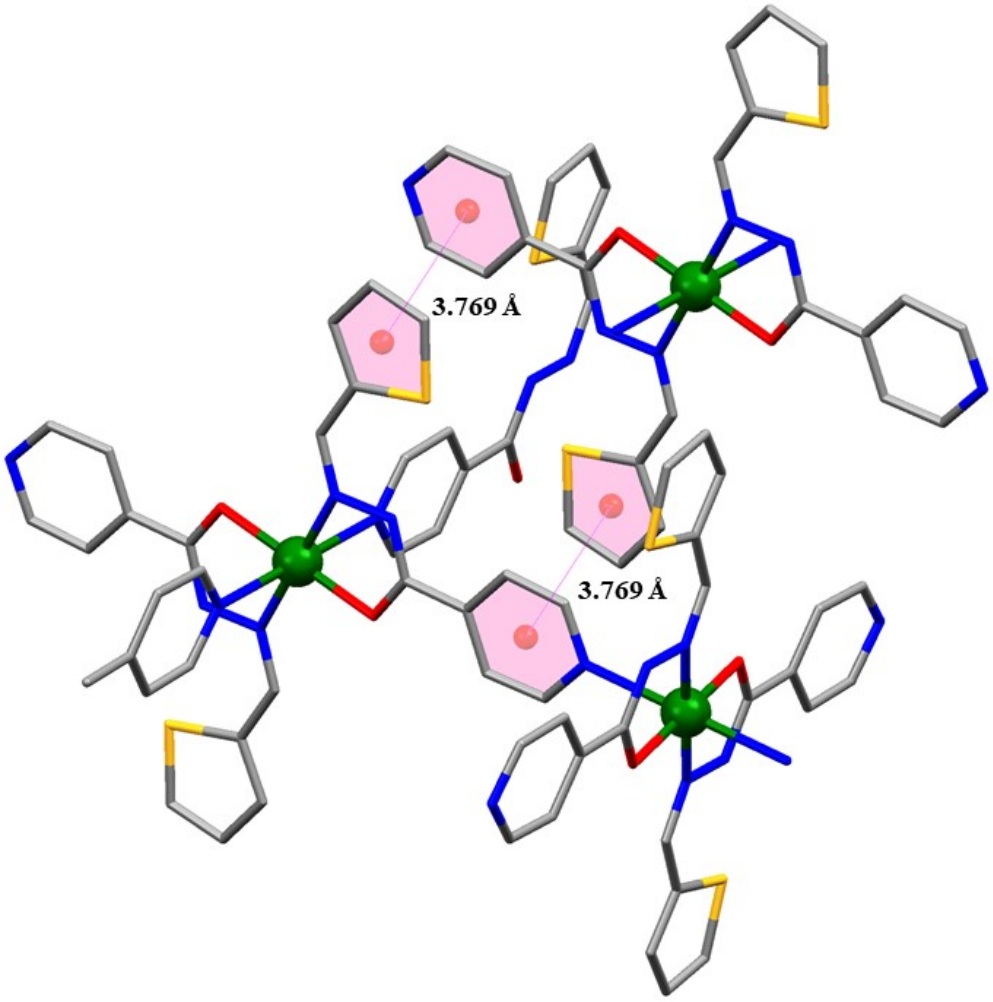

Fig. S3 π···π interaction in CP**1**.

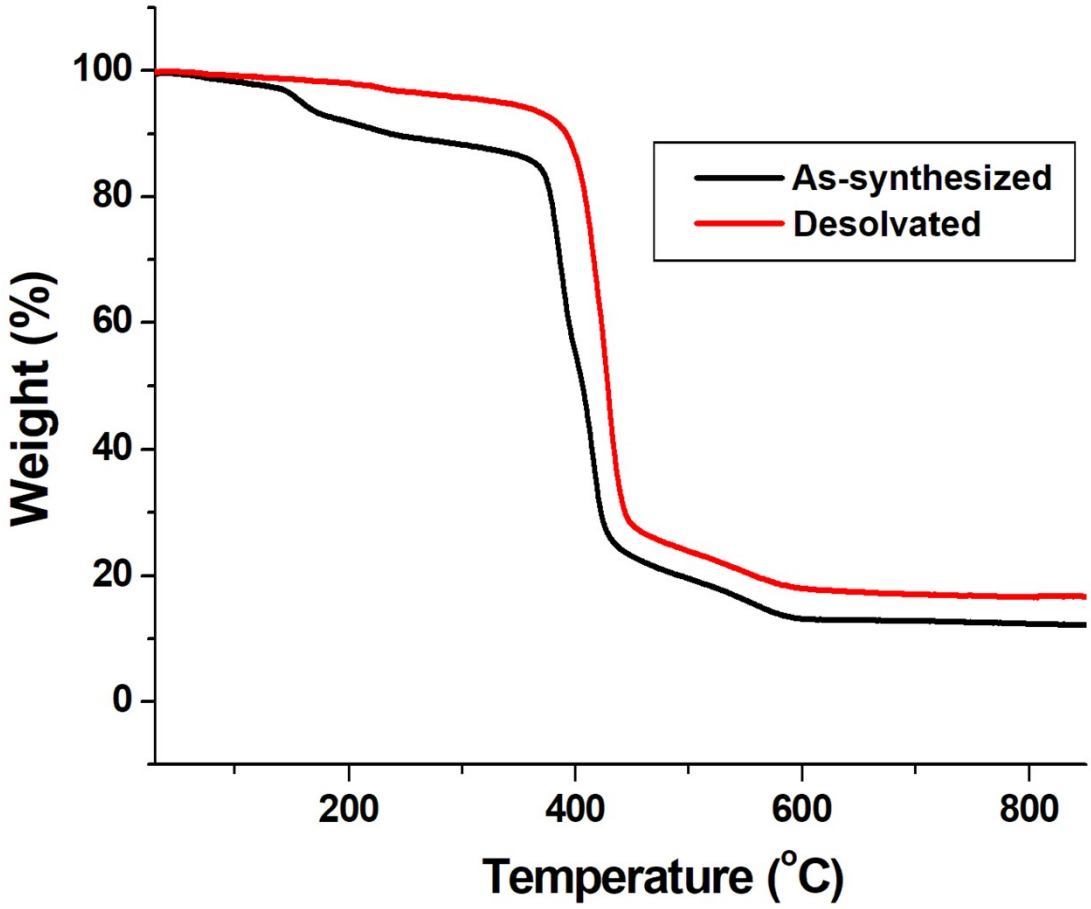

Fig. S4 TGA plot of CP**1**.

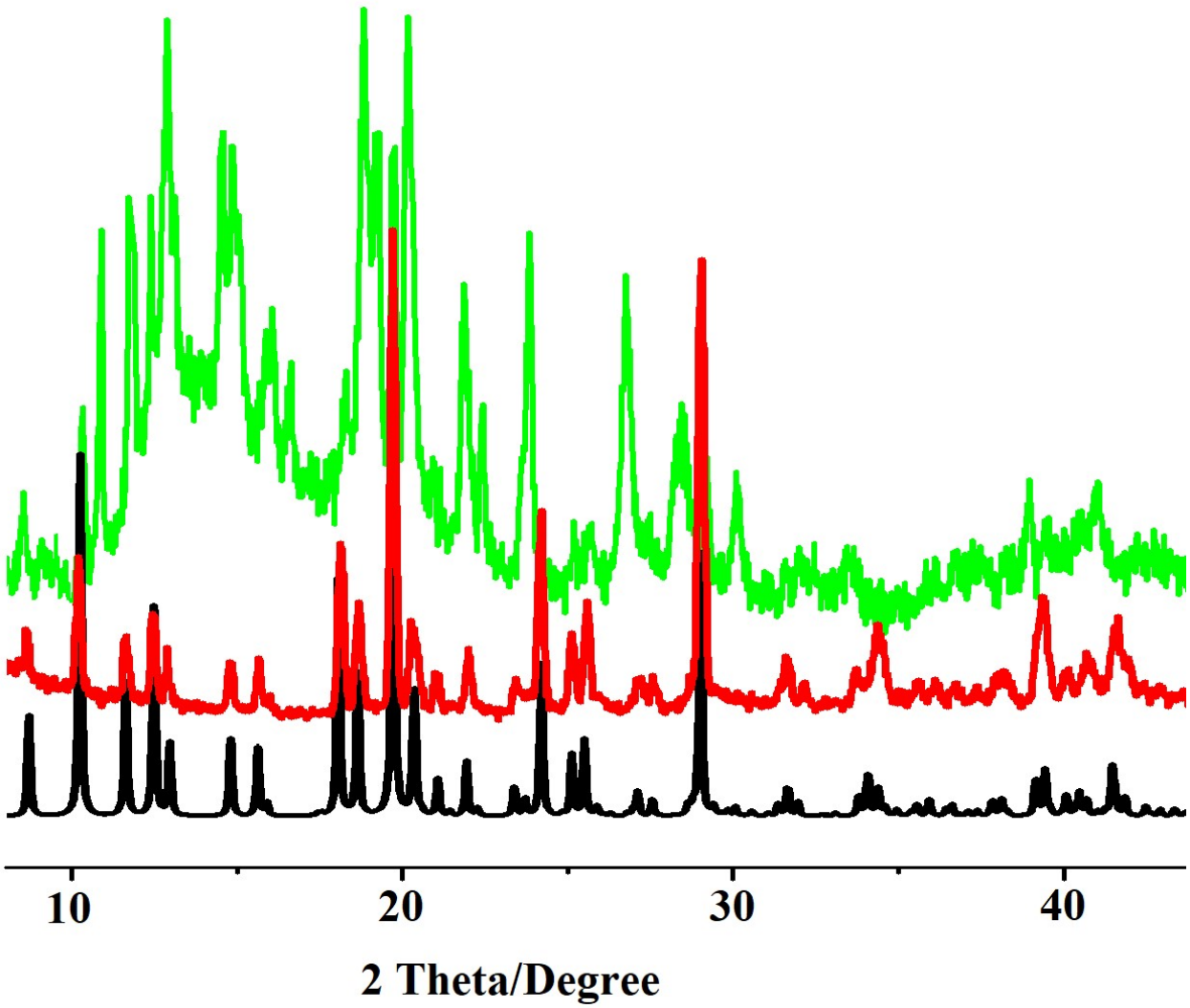

Fig. S5 Powder X-ray diffraction patterns of simulated CP**1** (black), as-synthesized (red) and desolvated (green).

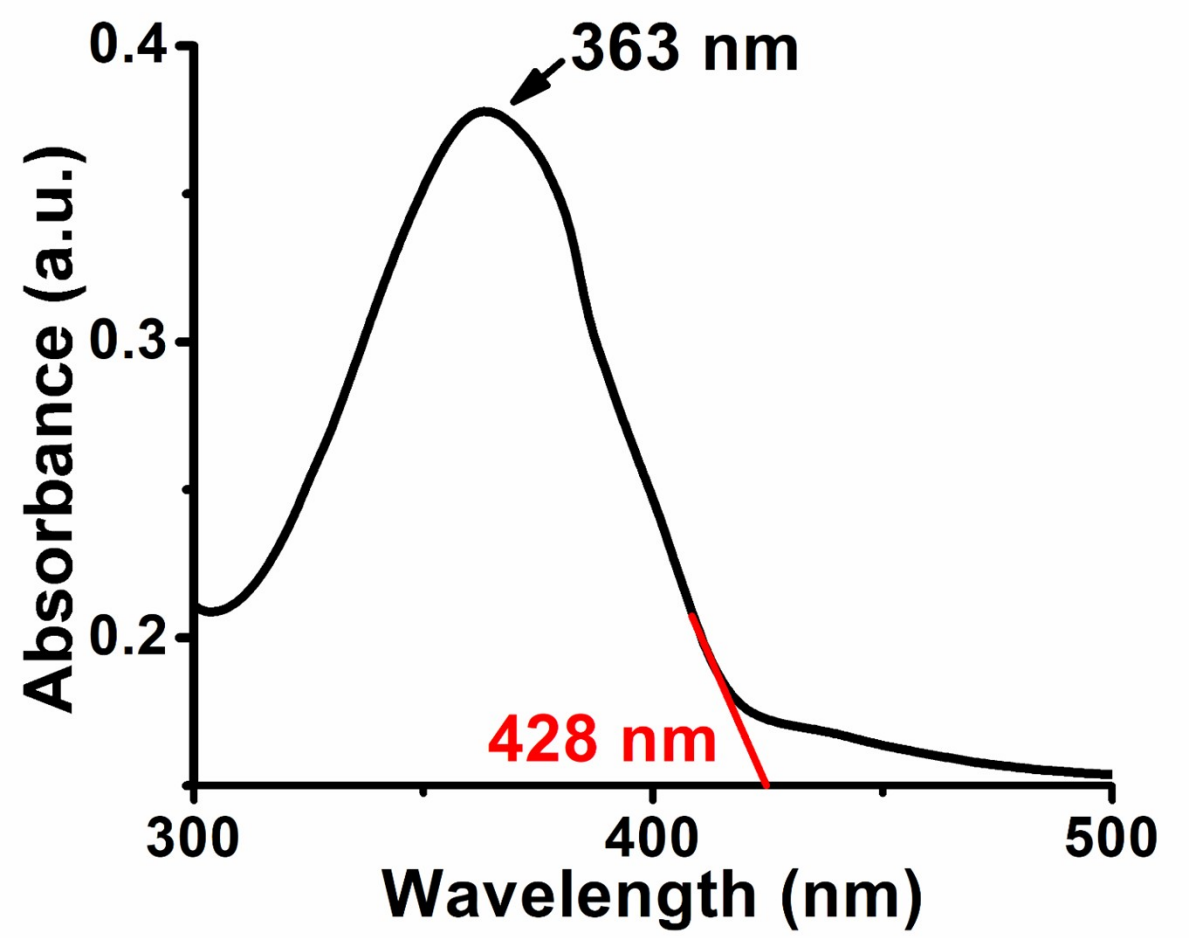

Fig. S6 Absorption spectrum of CP1 in DMF.

Table S3 Values of conductivity of CP1 based thin film device of different thickness.

Thickness (μm)	Conductivity of CP1 (S m^{-1})	
	Dark	Light
0.8	2.51×10^{-9}	5.94×10^{-5}
1.0	2.53×10^{-9}	5.97×10^{-5}
1.2	2.52×10^{-9}	5.98×10^{-5}
1.4	2.54×10^{-9}	5.96×10^{-5}

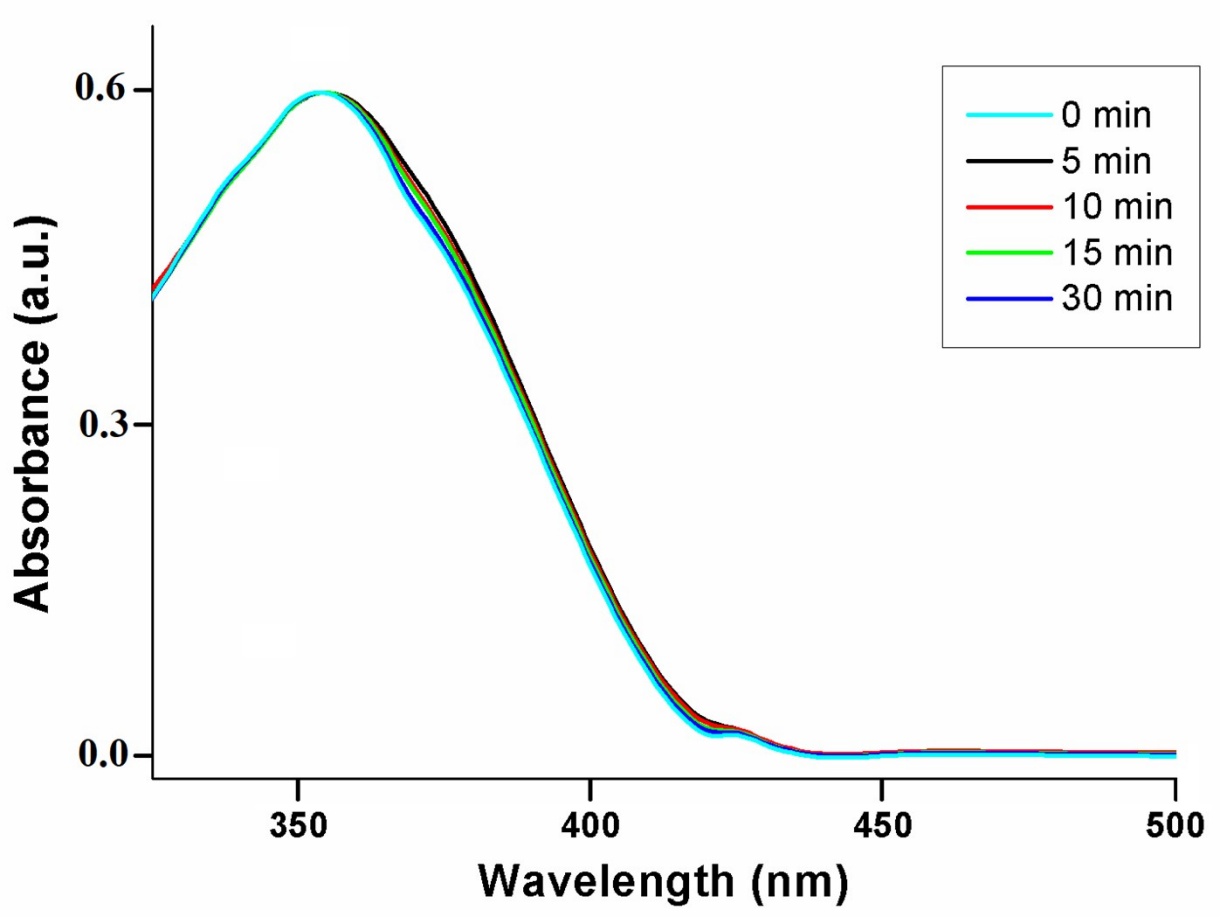

Fig. S7 Absorption spectra of CP**1** in 5% DMSO/H_2O after UV exposure (λ_{ex} = 365 nm) at different time interval.

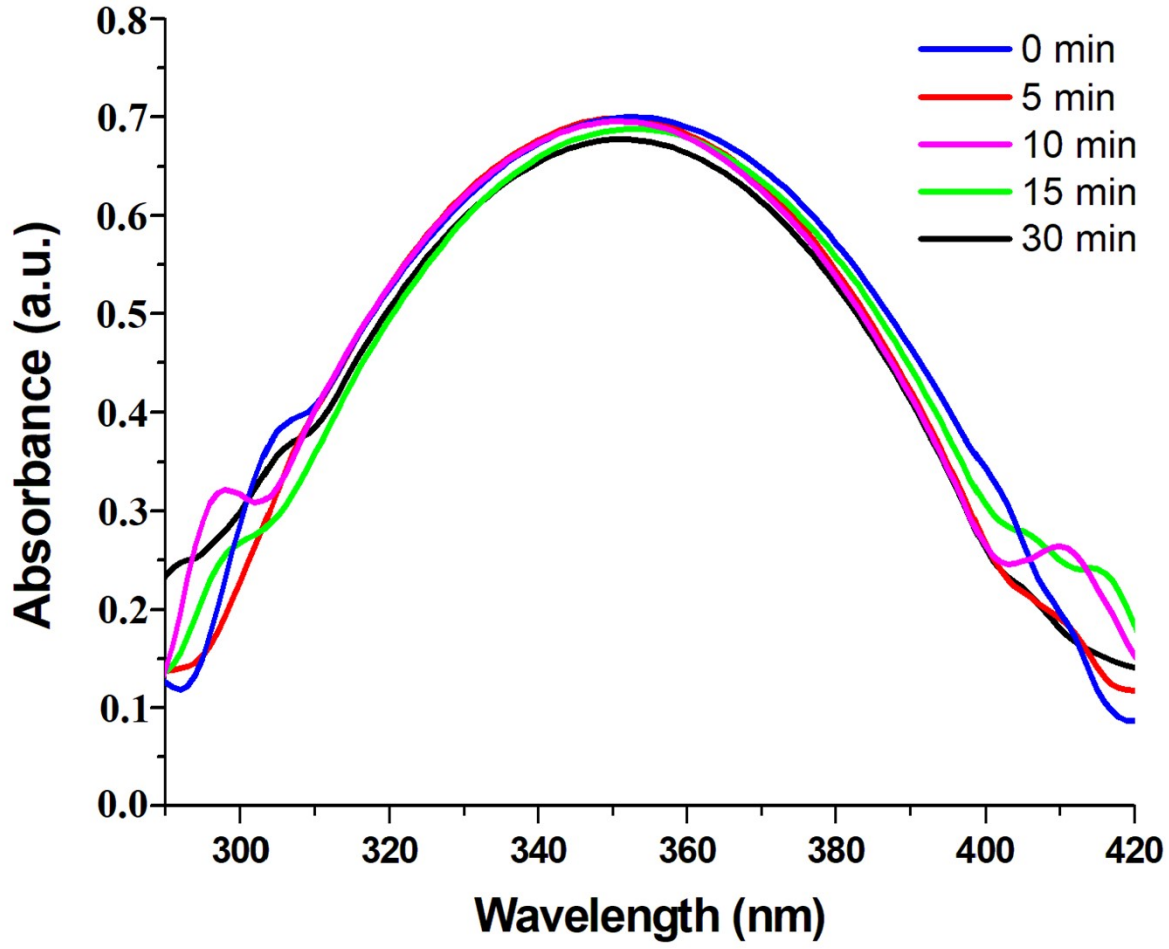

Fig. S8 Absorption spectra of CP**1** in solid state after UV exposure (λ_{ex} = 365 nm) at different time interval.

Table S4 Determination of turbidity (bacterial growth) by OD at 600 nm.

SL No.	**Concentration (µg/mL)**	**O.D[a] (a.u.)**
1.	Blank	0.025
2.	Control	0.693
3.	10	0.310
4.	20	0.085

5.	40	0.033
6.	60	0.031
7.	80	0.029
a. Average of three sets of experiments		

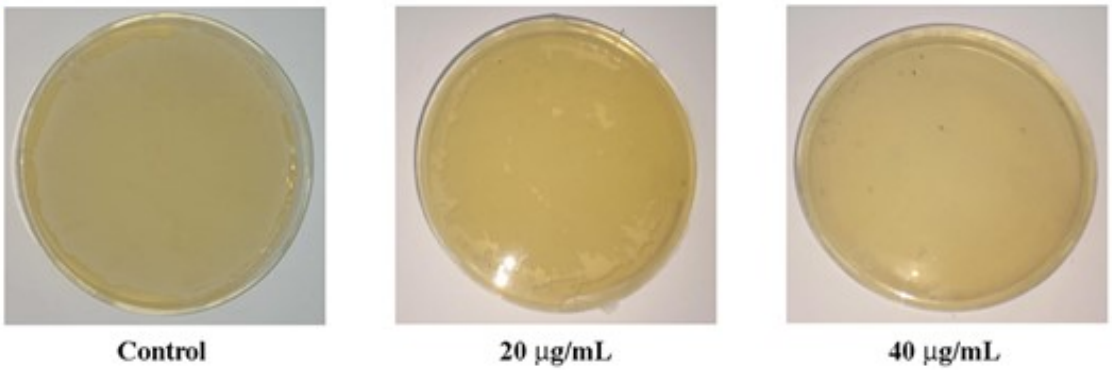

Fig. S9 Determination of MBC of MIC at just higher concentration of MIC of CP**1** (20 and 40 µg/mL) against *Staphylococcus aureus* by broth dilution assay.

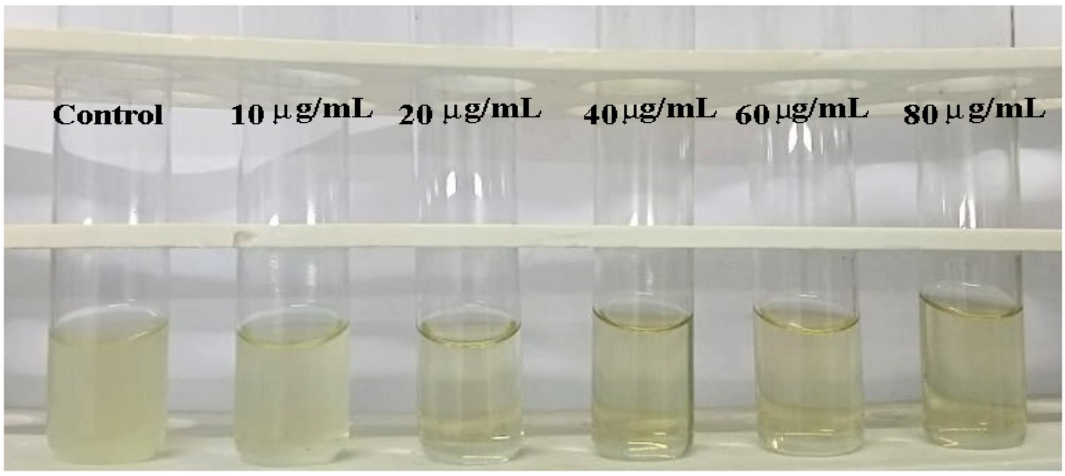

Fig. S10 Determination of Minimum Inhibitory Concentration of CP**1**: Different increasing concentration (10, 20, 40, 60, 80 µg/mL) were added separately against *Escherichia coli* by using the broth dilution method.

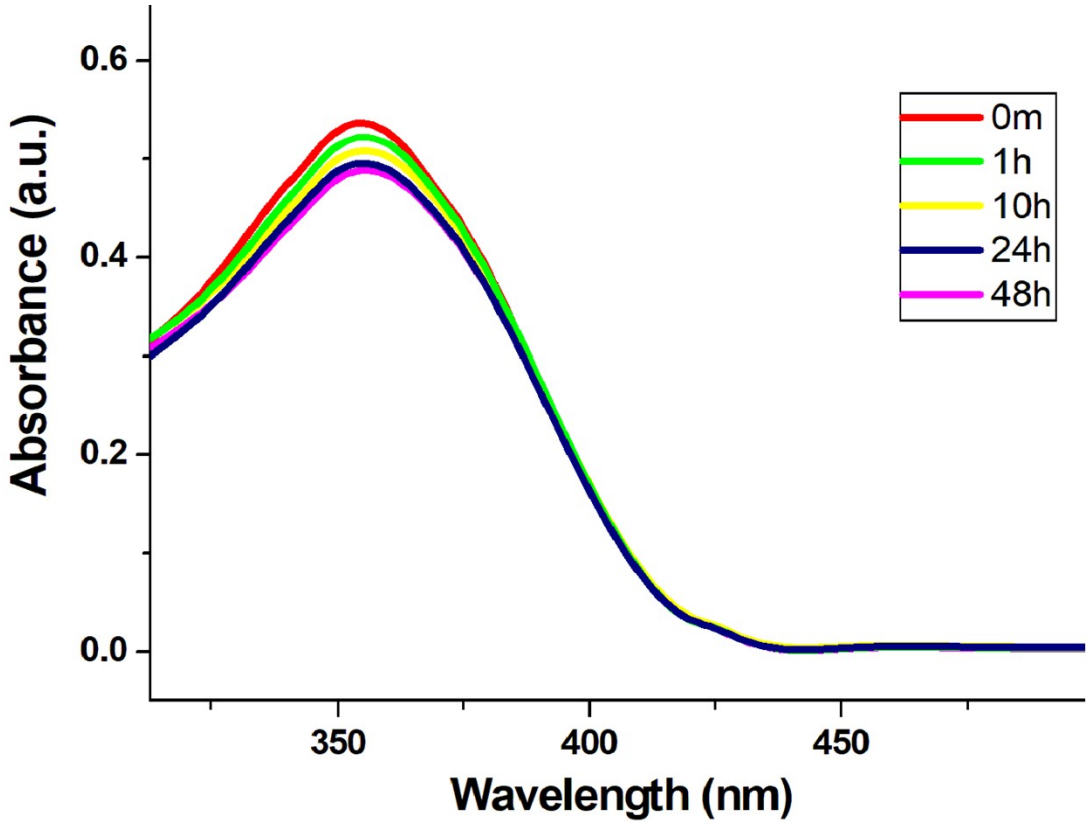

Fig. S11 Absorption spectra of CP**1** in 5% DMSO/H_2O at different time interval.

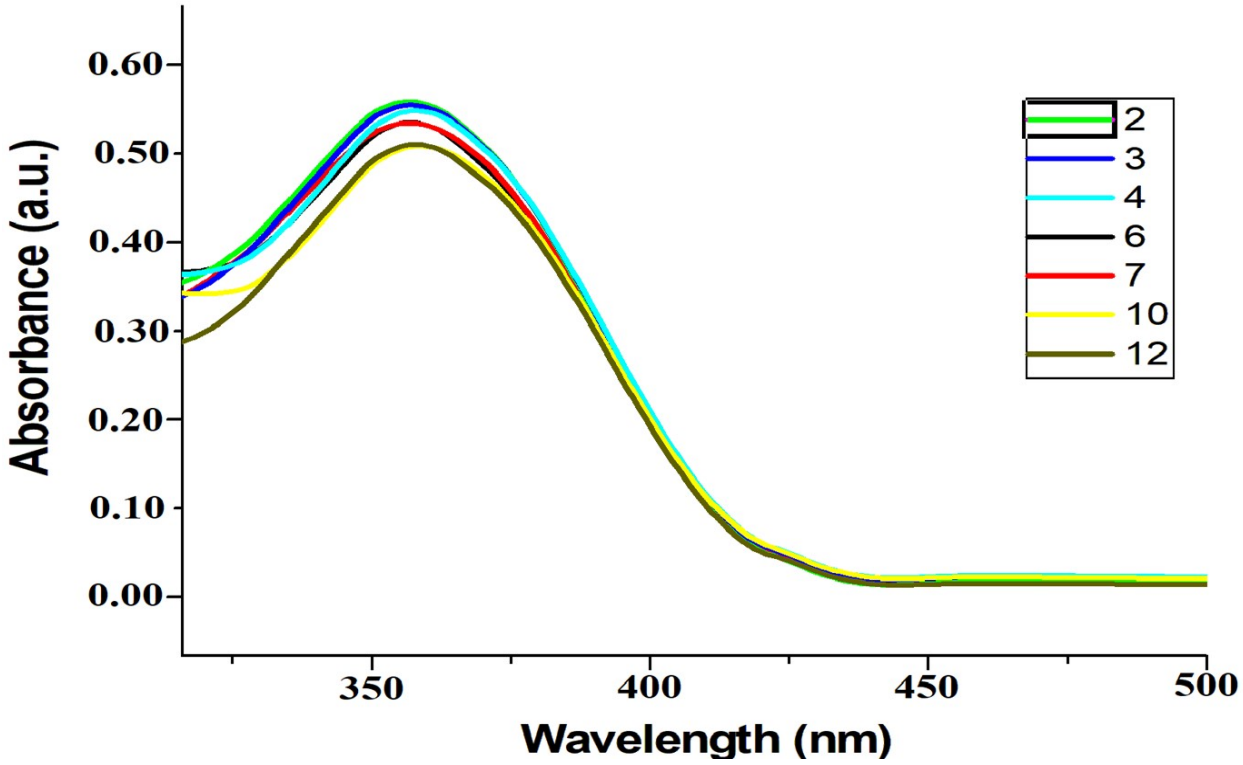

Fig. S12 Absorption spectra of CP**1** at different pH.

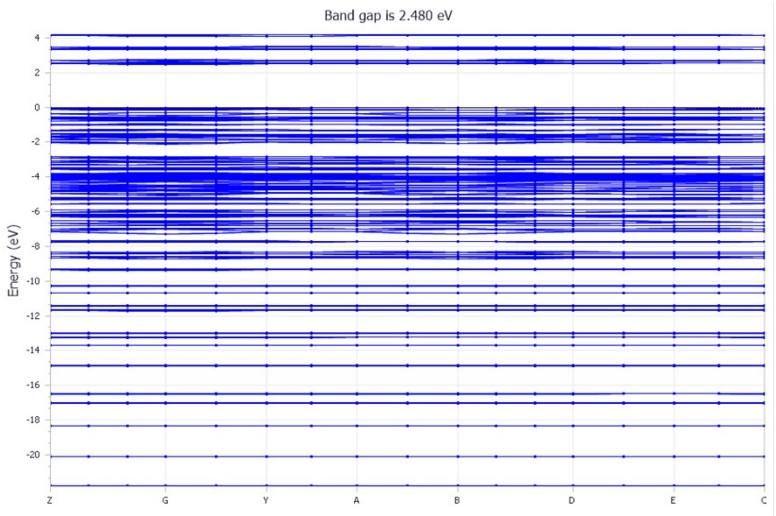

Fig. S13 The total unprocessed graphs for CP1.

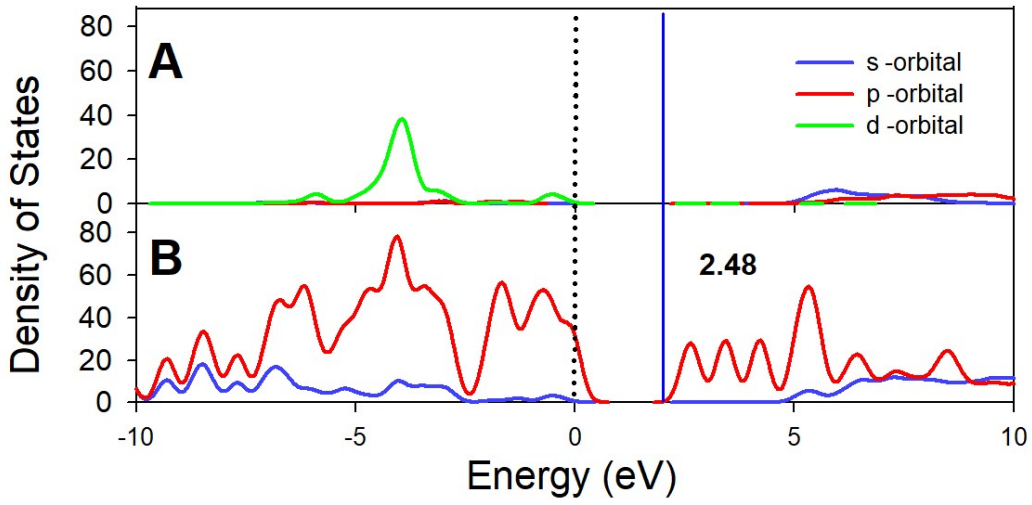

Fig. S14 The density states of different participating atomic orbitals in crystal cell, involving s-character (indicated by blue line), p-character (indicated by red line) and d-character (indicated by green line), calculated totally as well partially for (A) Zn atoms and (B) HSIZ ligand.

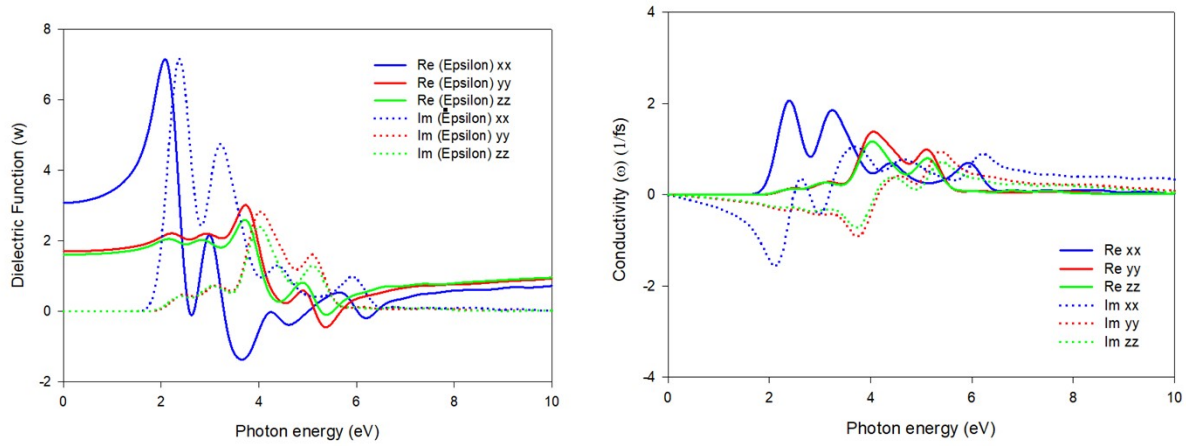

Fig. S15 Variations in dielectric function (left) and optical conductivity (right) of the crystal with respect to the photon energy. The solid and dotted lines denote the real and imaginary parts of the respective functions accordingly. Meanwhile, the polarized photon radiation has been directed incidentally towards x- (blue), y-(red) and z-(green) coordinates in the crystal.

Crystal Face	HOMO	LUMO
AB	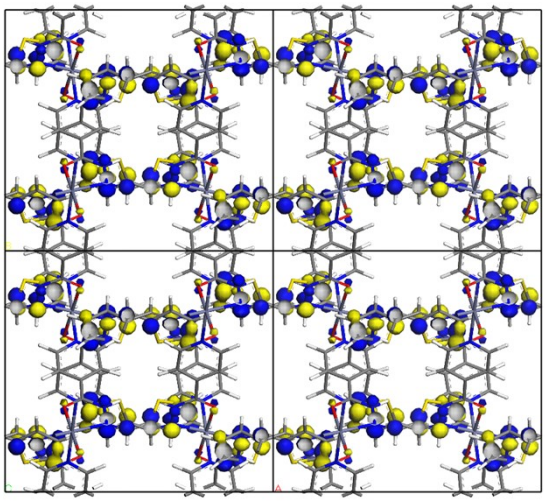	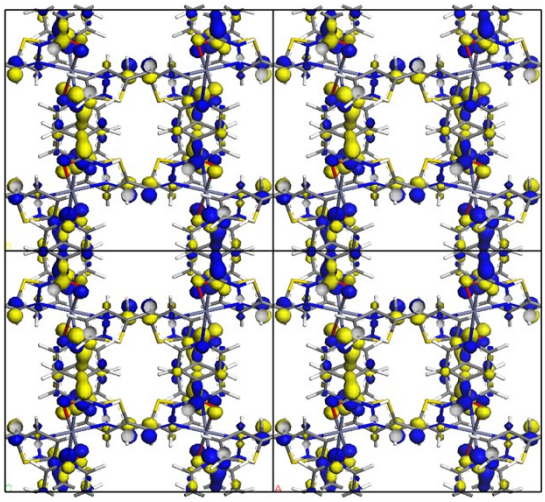
AC	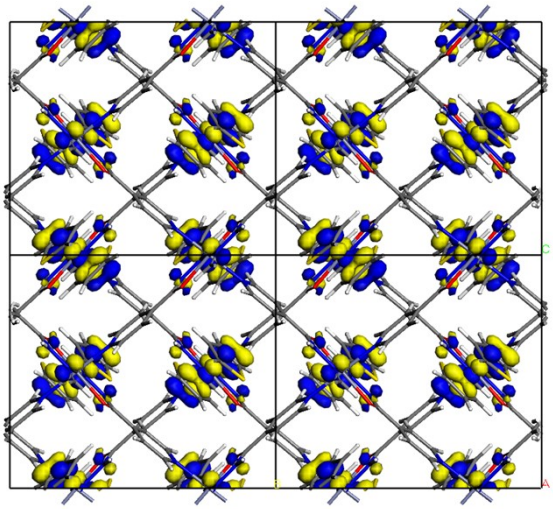	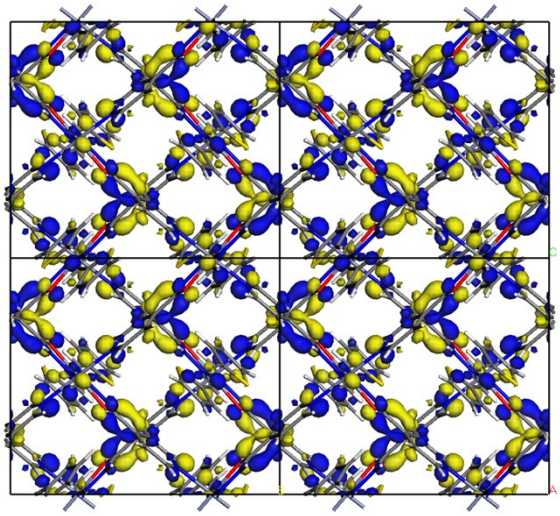

Fig. S16 Representation of HOMO, and LUMO orbitals in CP1 in the AB and AC crystal faces.

The orbitals are represented using the 0.025 a.u. isovalue and a 2 × 2 × 2 super cell.

Table S5 Comparison of dual-action from CP1 with previously reported coordination polymers.

Sl. No	Compound	Electrical conductivity under light illumination (S m^{-1})	Increase in conductivity with light illumination (fold)	Mobilities in light (m^2 V^{-1} s^{-1})	Biological study (Yes/No)	Ref.
1.	$[Cd(adc)(4\text{-phpy})_2(H_2O)_2]_n$	3.04×10^{-7}	1.98	9.15×10^{-7}	No	21
2.	$[Zn(adc)(4\text{-phpy})_2(H_2O)_2]_n$	7.78×10^{-8}	1.31	5.44×10^{-7}	No	21
3.	$[Cd_2(L_1)_2(NCS)_2(CH_3OH)]_n$	6.72×10^{-5}	53.33	9.04×10^{-12}	No	22
4.	$\{[Cd(HL_1)_2(N(CN)_2)_2]\cdot H_2O\}_n$	6.15×10^{-7}	3.45	1.42×10^{-12}	No	22
5.	$[Cd(HL_2)_2(N(CN)_2)_2]_n$	2.44×10^{-7}	2.28	1.04×10^{-12}	No	22
6.	$C_{40}H_{34}Cu_2N_6O_{18}$ (Cu-MOF1)	4.34×10^{-6}	2.14	6.54×10^{-12}	No	23
7.	$C_{20}H_{18}CuN_2O_{10}$ (Cu-MOF2)	7.60×10^{-6}	3.24	8.45×10^{-12}	No	23
8.	$[Pb_2(bdc)_{1.5}(aiz)]_n$	6.12×10^{-6}	2.08	1.38×10^{-6}	No	1
9.	$[Pb_2(bdc)_{1.5}(aiz)(MeOH)_2]_n$	3.66×10^{-7}	1.25	3.67×10^{-7}	No	1
10.	$[CdL_3(l\text{-}1,3\text{-}SCN)_2]_n$	2.16×10^{-8}	2.13	-	No	24
11.	$[Co(3\text{-}clpy)_2(fum)_2(H_2O)_2]_n$	4.84×10^{-6}	-	-	No	25
12.	$[Ni(L_4)(NCS)_2]_n$	3.5×10^{-4}	5	-	No	26

13.	$[Ni(L_5)(NCS)_2]_n$	4.9×10^{-4}	24.5	-	No	26
14.	$[Cu(fum)(4\text{-phpy})_2(H_2O)]$	6.13×10^{-6}	-	3.36×10^{-4}	No	27
15.	$\{[Zn(SIZ)_2].DMF\}_n$	5.97×10^{-5}	23596	6.83×10^{-5}	Yes	This work

Where, H_2adc= acetylenedicarboxylic acid, 4-phpy= 4-phenylpyridine, HL_1 = 2-Methoxy-6-((quinolin-3-ylimino)methyl)phenol, HL_2 = 2-Methoxy-6-((quinolin-5-ylimino)methyl)phenol], H_2bdc = 1,4-benzene dicarboxylic acid, aiz = (E)-N′-(thiophen-2-ylmethylene)isonicotinohydrazide), HL_3 = 2-(2-(ethylamino)ethyliminomethyl)-6-ethoxyphenol, 3-clpy = 3-Chloropyridine, H_2fum = fumaric acid, L_4 = Pyridin-2-ylmethylene-quinolin-8-yl-amine, L_5 = (6-Methyl-pyridin-2-ylmethylene)-quinolin-8-yl-amine,

HSIZ = (E)-N'-(thiophen-2-ylmethylene)isonicotinohydrazide, DMF=N,N-Dimethylformamide

References

1 S. Dey, S. Sil, B. Dutta, K. Naskar, S. Maity, P. P. Ray and C. Sinha, *ACS Omega*, 2019, **4**, 19959–19968.

2 G. M. Sheldrick, *Acta Crystallogr. Sect. A: Found. Adv.*, 2015, **71**, 3–8.

3 SMART and SAINT; Bruker AXS Inc.: Madison, WI, 1998.

4 G. M. Sheldrick, *Acta Crystallogr., Sect. A: Found. Crystallogr.*, 2008, **64**, 112–122.

5 L. J. Farrugia, *J. Appl. Crystallogr.*, 1997, **30**, 565–565.

6 A. L. Spek, PLATON: Molecular Geometry Program; University of Utrecht: Utrecht, The Netherlands, 1999.

7 S. J. Clark, M. D. Segall, C. J. Pickard, P. J. Hasnip, M. I. J. Probert, K. Refson and M. C. Payne, *Z. Kristallogr.*, 2005, **220**, 567–570.

8 J. P. Perdew, K. Burke and M. Ernzerhof, *Phys. Rev. Lett.*, 1996, **77**, 3865–3868.

9 J. P. Perdew, J. A. Chevary, S. H. Vosko, K. A. Jackson, M. R. Pederson, D. J. Singh and C. Fiolhais, *Phys. Rev. B.*, 1992, **46**, 6671–6687.

10 D. Vanderbilt, *Phys. Rev. B*, 1990, **41**, 7892–7895.

11 D. D. Koelling and B. N. Harmon, *J. Phys. C: Solid State Phys.*, 1977, **10**, 3107–3114.

12 S. Grimme, *J. Comput. Chem.*, 2006, **27**, 1787–1799.

13 F. Ahmed, J. Ortega-Castro, A. Frontera and M. H. Mir, *Dalton Trans.*, 2021, **50**, 270–278.

14 B. Delley, *J. Chem. Phys.*, 1990, **92**, 508–517.

15 J. M. Andrews, *J. Antimicrob. Chemother.*, 2001, **48**, 5–16.

16 P. R. Twentyman and M. Luscombe, *Br. J. Cancer*, 1987, **56**, 279–285.

17 T. Mosmann, *J. Immunol. Methods*, 1983, **65**, 55–63.

18 E. Miller, *Methods Mol. Med.*, 2004, **88**, 191–202.

19 E. Eruslanov and S. Kusmartsev, *Methods Mol. Biol.*, 2010, **594**, 57–72.

20 A. Dutta, D. Dhara, P. K. Parida, A. Si, R. Yesuvadian, K. Jana and A. K. Misra, *RSC Adv.*, 2017, **7**, 28853–28864.

21 F. Ahmed, J. Datta, B. Dutta, K. Naskar, C. Sinha, S. M. Alam, S. Kundu, P. P. Ray and M. H. Mir, *RSC Adv.*, 2017, **7**, 10369–10375.

22 P. Ghorai, A. Dey, A. Hazra, B. Dutta, P. Brandão, P. P. Ray, P. Banerjee and A. Saha, *Cryst. Growth Des.*, 2019, **19**, 6431−6447.

23 A. Hossain, A. Dey, S. K. Seth, P. P. Ray, P. Ballester, R. G. Pritchard, J. Ortega-Castro, A. Frontera and S. Mukhopadhyay, *ACS Omega*, 2018, **3**, 9160−9171.

24 S. Roy, A. Dey, P. P. Ray, J. Ortega-Castro, A. Frontera and S. Chattopadhyay, *Chem. Commun.*, 2015, **51**, 12974−12976.

25 S. Naaz, P. Das, S. Khan, B. Dutta, S. Maity, P. Ghosh, P. P. Ray, M. H. Mir, *Polyhedron*, 2021, **201**, 115159.

26 P. Ghorai, A. Dey, P. Brandão, S. Benmansour, C. J. G. García, P. P. Ray, A. Saha, *Inorg. Chem.*, 2020, **59**, 8749−8761.

27 F. Ahmed, S. Halder, B. Dutta, S. Islam, C. Sen, S. Kundu, C. Sinha, P. P. Ray, M. H. Mir, *New J. Chem.*, 2017, **41**, 11317−11323.